

Atrial proarrhythmias of ivabradine by inducing intracellular calcium overload and delayed afterdepolarizations in rabbit heart

Chengyu Wang¹, Mingjie Lin¹, Qiaomei Yang¹, Gang Li¹, Xiaoyan Liu¹, Qing Zhang¹, Shandong Yu¹, and Lin Wu¹

¹Peking University First Hospital

April 16, 2024

Abstract

Background: Ivabradine (IVA) inhibits hyperpolarization-activated cyclic nucleotide channel to reduce pacing current with a possible increasing risk of atrial fibrillation (AF). **Objective:** To determine the effects of IVA on atrial action potentials, atrial arrhythmic activities and intracellular calcium homeostasis. **Methods:** Langendorff-perfused hearts and atrial myocytes from New Zealand White rabbits were used to record 12-lead ECGs, left atrial monophasic APs and Ca²⁺ sparks. Ca²⁺ handling related protein from left atrium were tested using western blotting. **Results:** IVA (0.1-10 μM) slowed the HR and prolonged the atrial MAPD₉₀ (n=8, p<0.05) and induced atrial arrhythmias in 26% and 77% of hearts paced at cycle lengths of 350 ms and 570 ms, respectively (n=23 and 13, p<0.05). In hearts treated with either 0.3 μM acetylcholine (ACh) or 2 nM ATX-II with modulated atrial MAPDs, IVA (0.1-10 μM) caused either shortening or prolongation of MAPD₉₀, respectively (n=18 and 21, p<0.05) and atrial arrhythmias in 61.9% and 44.4% of hearts (p<0.05). IVA induced delayed afterdepolarizations in 41.7%, 62.5% and 50% of cells in the absence and presence of either ATX-II or ACh, respectively (n=12, 8 and 8, p<0.05). IVA (0.03-3 μM) increased the frequency, amplitude and full width at half-maximum (n=22, p<0.05), and the expression of ryanodine receptor and Na⁺/Ca²⁺ exchanger with decreased sarcoplasmic reticulum calcium pump (n=4-5, p<0.05). **Conclusion:** IVA caused a blunted HR reduction and increased atrial proarrhythmic risk in hearts with slow rate, enhanced vagal tone and late I_{Na}, and DADs resulting from enhanced Ca²⁺ release.

Atrial proarrhythmias of ivabradine by inducing intracellular calcium overload and delayed afterdepolarizations in rabbit heart

Chengyu Wang, PhD, Mingjie Lin, PhD, Qiaomei Yang, MD, Gang Li, MD, PhD, Xiaoyan Liu, MD, PhD, Qing Zhang, MD, PhD, Shandong Yu, MD, PhD, and Lin Wu, MD

Department of Cardiology, Peking University First Hospital, 8 Xishiku Street, West District, 100034, Beijing, China

Running Title: Ivabradine induces atrial arrhythmias

Corresponding author: Lin Wu, MD, Department of Cardiology, Peking University First Hospital, No. 8, Xishiku Street, West District, Beijing, 100034, China.

Tel: 86-10-83575799

E-mail: lin_wu@163.com

Number of text pages: 20

Number of tables: 3

Number of figures: 7

Number of references: 33

Number of words in the Abstract: 245

Number of words in the Introduction: 345

Number of words in the Discussion: 1408

Abbreviations: IVA, ivabradine; HCN, hyperpolarization-activated cyclic nucleotide; AF, atrial fibrillation; AP, action potential; ATX-II, anemone toxin-II; ACh, acetylcholine; LAM, left atrial myocyte; MAP, monophasic AP; ERP, atrial effective refractory period; PRR, post-repolarization refractoriness; APA, AP amplitude; V_{\max} , maximum upstroke velocity of the AP; DAD, delayed afterdepolarization; EAD, early afterdepolarization; FWHE, full width at half-maximum; FDHM, full duration at half-maximum; RyR, ryanodine receptor; NCX, $\text{Na}^+/\text{Ca}^{2+}$ exchanger; SERCA, sarcoplasmic reticulum calcium pump.

Recommended section assignment: Cardiac EP and pharmacology

Abstract

Background: Ivabradine (IVA) inhibits hyperpolarization-activated cyclic nucleotide channel to reduce pacing current with a possible increasing risk of atrial fibrillation (AF). **Objective:** To determine the effects of IVA on atrial action potentials, atrial arrhythmic activities and intracellular calcium homeostasis. **Methods:** Langendorff-perfused hearts and atrial myocytes from New Zealand White rabbits were used to record 12-lead ECGs, left atrial monophasic APs and Ca^{2+} sparks. Ca^{2+} handling related protein from left atrium were tested using western blotting. **Results:** IVA (0.1-10 μM) slowed the HR and prolonged the atrial MAPD_{90} ($n=8$, $p < 0.05$) and induced atrial arrhythmias in 26% and 77% of hearts paced at cycle lengths of 350 ms and 570 ms, respectively ($n=23$ and 13, $p < 0.05$). In hearts treated with either 0.3 μM acetylcholine (ACh) or 2 nM ATX-II with modulated atrial MAPDs, IVA (0.1-10 μM) caused either shortening or prolongation of MAPD_{90} , respectively ($n=18$ and 21, $p < 0.05$) and atrial arrhythmias in 61.9% and 44.4% of hearts ($p < 0.05$). IVA induced delayed afterdepolarizations in 41.7%, 62.5% and 50% of cells in the absence and presence of either ATX-II or ACh, respectively ($n=12$, 8 and 8, $p < 0.05$). IVA (0.03-3 μM) increased the frequency, amplitude and full width at half-maximum ($n=22$, $p < 0.05$), and the expression of ryanodine receptor and $\text{Na}^+/\text{Ca}^{2+}$ exchanger with decreased sarcoplasmic reticulum calcium pump ($n=4-5$, $p < 0.05$). **Conclusion:** IVA caused a blunted HR reduction and increased atrial proarrhythmic risk in hearts with slow rate, enhanced vagal tone and late I_{Na} , and DADs resulting from enhanced Ca^{2+} release.

Key words: ivabradine, atrium, proarrhythmia, delayed afterdepolarization, Ca^{2+} spark

Introduction

Drug-induced cardiac arrhythmias, especially proarrhythmic effects of class I and III antiarrhythmic drugs, are common in patients with structural heart diseases and remain an important issue for the development and clinical use of drugs. With the high prevalence of atrial fibrillation (AF), drug-induced AF becomes a problem worthy of clinical attention because of the potentially high incidence and poor understanding on the underlying mechanisms^{1, 2}. Many cardiovascular and on-cardiovascular drugs are associated with increased risk of AF in clinic. Ivabradine (IVA), a class 0 antiarrhythmic agent in the modernized classification of cardiac antiarrhythmic drug³, selectively inhibits hyperpolarization-activated cyclic nucleotide (HCN) channel to reduce the pacemaker funny current (I_{f}) in the sinus node and is used to treat inappropriate sinus tachycardia in addition to or as an alternative to digitalis, β blockers or calcium channel inhibitors⁴ without affecting blood pressure, myocardial contractility and atrioventricular nodal conduction. However, clinical use of IVA caused no reduction in cardiovascular mortality even when the sinus heart rate was already decreased to 70 beat per minute or lower in patients with heart failure and/or coronary artery diseases^{5, 6}.

HCN channels are highly expressed during embryonic atrial development, decrease gradually and are limited to the cardiac conduction system with age. HCN channels, especially the HCN2 and HCN4 channels, are re-expressed under pathophysiological conditions, including heart failure, myocardial infarction, hypertrophy and atrial arrhythmias⁷. Drug-induced AF is more common in patients with bradycardia from the use of

drugs to slow heart rate or in patients with increased vagal tone than others⁸. Clinical use of IVA is associated with a possibly 24% increase in the risk of developing AF⁹. The mechanisms, risk factors and the correlation with the prognosis underlying the increased susceptibility to AF following IVA application remain underdetermined. In this study, the atrial proarrhythmic activity of IVA was reproduced and the underlying mechanisms were investigated in isolated rabbit hearts and left atrial myocytes (LAMs). To the best of our knowledge, this is the first report to demonstrate that IVA has atrial proarrhythmic activities in experimental animal models.

Materials and Methods

Animals

Animal use in this study conformed to the “Guide for the Care and Use of Laboratory Animals” published by the US National Institutes of Health (NIH Publication No. 85-23, revised 2011) and was approved by the Institutional Animal Care and Use Committee of Peking University First Hospital (201879).

Electrophysiological study in rabbit isolated heart

New Zealand white female rabbits (weight 2.5-3.0 kg) were anesthetized using xylazine (16 mg/kg by IM, Huamu; China) and ketamine (40 mg/kg by IM, CAHG; China). Rabbit hearts were excised and placed in a modified Krebs-Henseleit (K-H) solution (pH=7.4, gassed with 95% O₂ and 5% CO₂) composed of the following (in mM; Sigma, USA): 118 NaCl, 2.8 KCl, 1.2 KH₂PO₄, 2.5 CaCl₂, 0.5 MgSO₄, 2.0 pyruvate, 5.5 glucose, 0.57 Na₂EDTA, and 25 NaHCO₃. The aorta was cannulated, and the heart was perfused at a rate of 20 mL/min with K-H solution warmed to 37 °C according to the Langendorff system. Coronary perfusion pressure was monitored from a side port of the aortic cannula. A bipolar Teflon-coated electrode was placed on the right atrial appendage to pace the heart with an electrical stimulator (EP-4, St. Jude Medical; USA), 0.6 ms in width and 3–5-fold threshold amplitude. The concentration-response relationships of IVA on heart rate were tested in spontaneously beating hearts, while monophasic APs (MAPs) and arrhythmic events in the atria were obtained from hearts paced at a fixed pacing cycle length (CL) of 350 ms or 570 ms for hearts after SANs were thermo-ablated. After 20-30 minutes of equilibrium, the hearts were randomly assigned into groups treated with either increasing concentrations (0.01-10 μM) of IVA at the spontaneous heart rate (HR) or paced to measure EP parameters at a fixed pacing cycle lengths of 350 ms and 570 ms, or in the absence and presence of low-concentration anemone toxin-II (ATX-II) or acetylcholine (ACh) to increase late sodium current (I_{Na}) or vagal tone and mimic the pathological conditions, respectively. ATX-II (2 nM) and ACh (0.3 μM) were confirmed not to cause atrial arrhythmias in any of the hearts studied, similar to our previous report¹⁰.

MAP, ECG and atrial arrhythmia recordings in isolated hearts

The atrial MAPs, pseudo-12-lead electrocardiograms (ECGs), and coronary perfusion pressure were continuously monitored and digitized in real time. Pressure-contact Ag-AgCl MAP electrodes were placed on the endocardium of left auricular appendage. Atrial MAP profiles were analyzed using software (Spike2 version 6.03, CED, UK) to determine the MAP duration at which repolarization was 90% completed (MAPD₉₀). The atrial effective refractory period (ERP) and arrhythmic events were induced by the S1S2 and S1S1 (burst protocol) programmed stimulations. ECG parameters were measured from a superimposition of 12-lead ECG recordings. Spontaneous sinus heart rate was measured from an average of 10 atrial beats when the rhythm was regular without arrhythmias.

An extra-atrial beat (EAB) was defined as a spontaneous beat occurring earlier than the next regular (spontaneously beating heart) or pacing (paced heart) beat. Atrial tachycardia (AT) was defined as a sequence of three or more consecutive, relatively regular spontaneous atrial beats occurring unexpectedly at a rate exceeding the spontaneous or pacing rate. An episode of AF was defined as a sequence of fast, irregular atrial signals in MAP and ECG recordings with irregular QRS complexes in a 12-channel ECG record. ATs and AFs were collectively referred to as atrial arrhythmic events/arrhythmias. Post-repolarization refractory period (PRR) was calculated using an equation of (ERP – MAPD₉₀).

Isolation of LAMs

Single LAMs were enzymatically isolated from New Zealand White rabbits (weight 1.5-2.0 kg) as described in a previous study¹¹. In brief, hearts were removed rapidly and perfused with Ca²⁺-free Tyrode solution containing the following compounds (in mM; purchased from Sigma-Aldrich, MA, USA): 135 NaCl, 5.4 KCl, 1.0 MgCl₂, 10 glucose, 0.33 NaH₂PO₄, and 10 HEPES) at pH=7.4 with NaOH for 5-10 minutes to washout blood. Then, the hearts were perfused with Ca²⁺-free Tyrode solution containing collagenase type I (0.5 g/L) and bovine serum albumin (BSA, 1.0 g/L) for 30-40 minutes before being perfused with KB solution, which contained the following compounds (in mM): 70 KOH, 40 KCl, 20 KH₂PO₄, 50, glutamic acid, 20 taurine, 0.5 EGTA, 10 glucose, 10 HEPES, and 3.0 MgSO₄) at pH=7.4 titrated with KOH for another 5-10 minutes. After perfusion, the left atrium was collected and cut into small pieces gently in KB solution. LAMs were filtered through a cell strainer (mesh number 200) and stored in KB solution at room temperature. All solutions used in this study were saturated with 100% O₂ and were maintained at 37 °C.

Recordings of (action potential) AP and triggered activity in single atrial myocytes

Quiescent and Ca²⁺-tolerant atrial myocytes were selected for recording APs, delayed afterdepolarizations (DADs) and early afterdepolarizations (EADs) were elicited in the whole-cell patch-clamp configuration using a HEKA EPC-10 patch master amplifier. Atrial myocytes were bathed and perfused (2-3 ml/min) in a bath solution containing the following reagents (in mM; Sigma-Aldrich, MA, USA): 144 NaCl, 5.6 KCl, 1.2 MgCl₂, 5 HEPES, 1.8 CaCl₂, 11 Glucose at pH=7.4 titrated with NaOH and maintained temperature at 22-24 °C. The patch pipette solution contained the following reagents (in mM; Sigma, USA: 110 K-aspartate, 30 KCl, 5 NaCl, 10 HEPES, 0.1 EGTA, 5 Mg-ATP, 5 creatine phosphate, and 0.05 cAMP) at pH=7.2 titrated with KOH. When filled with pipette solution, the electrode resistance was in the range of 3-5 MΩ. APs were induced in current-clamp mode by 1.5-fold diastolic threshold-current pulses of 5-ms duration at a 1000-ms pacing cycle lengths. EADs were elicited by changing the stimulation frequency to 0.25 Hz, and DADs were determined following a baseline pacing CL of 9000 ms and 15 beats with a stimulation frequency of 2.5 Hz.

Recording of Ca²⁺ sparks in atrial myocytes using confocal imaging

Atrial myocytes were bathed in an internal solution composed of (in mM; Sigma, USA) 135 NaCl, 5.4 KCl, 1.0 MgCl₂, 1.8 CaCl₂, 10 glucose, 0.33 NaH₂PO₄, and 10 HEPES, pH=7.4, with NaOH and incubated in 10 μM Fluo-4 AM for 20 minutes (Thermo Fisher Scientific; USA). A laser-scanning confocal microscope system (TCS SP5; Leica; Germany) with a 20× water-immersion objective was applied to acquire Ca²⁺ sparks. Fluo-4 AM was excited at 488 nm with an Ar laser. Myocytes were placed with their long axes within ±10 degrees of the cell and approximately equidistant between the outer edge of the cell and the nuclei to ensure that the nuclear area was not included in the scan line. All experiments were performed at room temperature (22-24 °C). Sparks were analyzed with SparkMaster¹², and the number, frequency (sparks/100 μm/s, Ca²⁺ release events), amplitude ($\Delta F/F_0$), full width at half-maximum (FWHM, μm) and full duration at half-maximum (FDHM, ms) of the detected sparks were obtained. To exclude false positive events, a threshold criterion for spark detection of 3.8 was chosen for data analysis. F₀ was the initial fluorescence recorded under steady-state conditions. Spark amplitudes and widths were determined based on the Ca²⁺ released during individual sparks.

Western blotting

Left atrial tissues were collected after isolated heart perfusion, and were homogenized using a tissue lyser. Levels of RyR2 (ryanodine receptor, LS-C93425, LifeSpan BioSciences, USA), SERCA2 (sarcoplasmic reticulum calcium pump, 4388s, Cell Signaling Technology, USA) and NCX1 (Na⁺/Ca²⁺ exchanger, 5507-I-AP, Proteintech, USA) were determined by western blotting as our previous study¹³.

Statistical analyses

Data are reported as the means ± standard errors of the means (SEMs). Statistical analysis was performed using IBM SPSS Statistics for Windows (version 20.0, IBM, New York, USA). The concentration-response relationships were analyzed using GraphPad Prism for Windows (version 6.02, GraphPad Software, Inc.,

San Diego, CA). When control/baseline and treatment values were obtained from the same heart/cell, the significance of the differences in the measures before and after interventions was determined by repeated measures one-way ANOVA followed by the Newman-Keul test. The χ^2 test and Fisher's test were used to compare the incidences of atrial arrhythmias and trigger activities. Differences were considered significant at $p < 0.05$.

Results

IVA decreased spontaneous intrinsic HR in isolated rabbit hearts

The HR and PR intervals at baseline of the isolated rabbit hearts were 161.90 ± 2.81 bpm and 42.84 ± 3.02 ms, respectively ($n=24$). IVA (0.1-10 μM) reduced the HR by 83.24 ± 7.30 in a concentration-dependent manner from 161.90 ± 2.81 bpm to 81.14 ± 5.15 bpm at concentration of or higher than 0.1 μM and prolonged the PR interval from 44.12 ± 3.77 ms to 61.96 ± 3.50 ms at concentration of or higher than 1 μM ($n=8$, $p < 0.05$; Fig 1 and Table 1). At concentrations of 6 and 10 μM , IVA prolonged QT interval and QRS duration from 212.00 ± 3.56 ms and 62.00 ± 2.03 ms to 218.49 ± 2.87 and 76.22 ± 15.19 , and 220.16 ± 6.94 and 80.46 ± 7.33 ms, respectively ($n=8$, $p < 0.05$). ATX-II (2 nM) and ACh (0.3 μM) caused a small decrease in HR from 4.87 ± 1.59 and 10.34 ± 3.89 bpm, respectively. However, in the continued presence of either ATX-II or ACh, IVA caused a smaller decrease in HR by 58.07 ± 6.09 bpm and 49.14 ± 5.50 bpm ($p < 0.05$ vs. in absence of either ATX-II or ACh, Fig 1).

IVA changed atrial MAPD₉₀, ERP and PRR in paced hearts

IVA, at high concentrations of 10 μM , prolonged the MAPD₉₀, ERP and PRR when hearts were paced a CL of 570 ms to maintain a stable heart rate before and after IVA infusion from 50.59 ± 2.55 , 92.50 ± 5.23 and 44.29 ± 3.03 ms to 58.93 ± 1.21 , 126.25 ± 7.14 and 68.57 ± 5.52 ms ($n=13$, $p < 0.05$ vs. baseline; Fig 2A-a). When the hearts were paced at CL of 350 ms, IVA (0.3-10 μM) significantly prolonged atrial MAPD₉₀ from 47.62 ± 1.72 to 62.08 ± 3.01 ms ($n=13$, $p < 0.01$; Fig. 2A), IVA at high concentrations of 3-10 μM prolonged the ventricular epi-cardial MAPD₉₀ from 127.38 ± 4.37 ms to 151.27 ± 1.53 ms ($n=6$, $p < 0.01$), respectively.

ATX-II (2 nM) and ACh (0.3 μM) caused either prolongation or shortening of MAPD₉₀, ERP and PRR, respectively, from 47.62 ± 1.72 , 85.00 ± 3.45 and 40.75 ± 3.45 ms to 68.95 ± 4.03 , 95.33 ± 2.76 and 22.83 ± 4.82 , and 32.06 ± 1.83 , 70.33 ± 1.09 and 38.33 ± 2.09 ms ($n=18$ and 21 , respectively, $p < 0.05$, Fig 2B-C). IVA (1-10 μM) prolonged the MAPD₉₀ in control hearts ($n=23$, $p < 0.05$ vs. baseline; Fig 1A-a) and ACh-treated hearts ($n=21$, $p < 0.05$ vs. ACh alone; Fig 2C-a) but shortened the MAPD₉₀ in ATX-II-treated hearts ($n=18$, $p < 0.05$ vs. ATX-II alone; Fig 2B-a). For the ERP and PRR, IVA (1-10 μM) showed prolonging effects in all hearts ($p < 0.05$ vs. baseline or ATX-II/ACh alone; Fig 2-b and 2-c). These results suggest that the effect of IVA on atrial electric parameters depends on hearts' substrate in rabbits.

Effects of IVA on the action potentials of LAMs

IVA (0.3 μM) reduced the AP amplitude (APA) and maximum upstroke velocity of the AP (V_{max}) from 139.02 ± 5.43 mV and 187.47 ± 14.85 V/s to 128.03 ± 5.37 mV and 175.12 ± 14.73 V/s, $p < 0.05$ vs. baseline, Table 2), shortened APD₃₀ from 131.06 ± 4.17 to 111.00 ± 9.92 V/s ($n=12$, $p < 0.05$) without changing resting membrane potential (RMP). IVA (10 μM) reduced RMP (-72.45 ± 3.81 mV) and shortened the APD₅₀ and APD₉₀ ($n=12$, $p < 0.05$).

ATX-II (1 nM) slowed V_{max} , and prolonged APD₃₀, APD₅₀ and APD₉₀ ($n = 8$ cells/4 rabbits, $p < 0.05$ vs. 0 μM IVA, Table 3 and Fig 3A) without changing RMP and APA. In the presence of ATX-II, administration of IVA (0.3 and 3 μM) shortened the APD₃₀, APD₅₀ and APD₉₀ values from 159.67 ± 13.07 , 179.97 ± 20.69 and 260.94 ± 19.26 ms to 91.13 ± 23.85 , 122.71 ± 25.47 and 190.71 ± 29.52 ms ($p < 0.05$ vs. ATX-II alone), respectively. However, administration of ACh alone increased the myocytes' RMP from -78.83 ± 1.81 to -65.72 ± 3.61 mV, decreased the APA from 141.36 ± 1.98 mV to 123.78 ± 4.13 mV ($n = 8$, $p < 0.05$ vs. baseline, Table 3), and shortened the values of APD₃₀, APD₅₀ and APD₉₀ from 130.71 ± 17.68 , 153.83 ± 15.49 , and 220.34 ± 14.82 ms to 91.99 ± 17.60 , 142.04 ± 17.85 , and 146.47 ± 8.89 ms at most, respectively ($n =$

8s, $p < 0.05$ vs. baseline, Table 3) of LAMs. In the continued presence of ACh, IVA (0.3 and 3 μM) maximally prolonged the ACh-induced shortening of APD_{30} , APD_{50} and APD_{90} to 101.49 ± 17.61 , 131.85 ± 13.47 and 140.18 ± 5.15 ms, respectively ($p < 0.05$ vs. ACh alone). The present results indicate that IVA affects the depolarization of APs in atrial cells while influencing the whole AP process in ATX-II- and ACh-pretreated cells.

IVA caused atrial arrhythmias in hearts and DADs in LAMs

Atrial arrhythmias, specifically AF, was not observed and were induced by programmed stimulations in the presence of IVA in 6 of 23 hearts (26.1%, $p < 0.05$ vs. baseline) and 10 of 13 hearts (76.9%, $p < 0.05$ vs. baseline) in hearts paced at a basal CLs of 350 and 570 ms, respectively (Fig 4B). In contrast, in hearts paced at 350ms and pretreated with either 2 nM ATX-II or 0.3 μM ACh, IVA (0.03-10 μM) significantly increased the incidence of atrial arrhythmias in 8 of 18 (44.4%, $p < 0.05$ vs. ATX-II alone) or 13 of 21 (61.9%, $p < 0.05$ vs. ACh alone) hearts, respectively (Fig 4C). The atrial single-cell patch-clamp tests indicated that IVA (0.1-3 μM) induced DADs but not EADs with incidences of 41.7% (5/12), 62.5% (5/8) and 50.0% (4/8) in control, ATX-II- and ACh-treated cells, respectively (compared to baseline, $p < 0.05$, Fig 5A-B).

IVA altered the properties of Ca^{2+} sparks

Fig 6A depicts line-scan images of Fluo-4 AM fluorescence with the corresponding profiles of Ca^{2+} sparks. Under control conditions, the average Ca^{2+} spark frequency, amplitude, FWHM and FDHM were 2.68 ± 1.17 sparks/100 $\mu\text{m/s}$, 0.74 ± 0.45 , 0.48 ± 0.14 μm , and 29.81 ± 7.63 ms ($n = 239$ sparks/22 cells), respectively. After IVA treatment, spark frequency, amplitude and FWHM gradually increased in concentration-dependent manners and FDHM remained unchanged (Fig 6B). IVA (0.3 μM) increased spark frequency, amplitude and width of Ca^{2+} spark by 1.9, 4.2 and 2.7 fold ($p < 0.05$ vs. baseline), respectively. These results suggest that IVA mainly affects the spatial characteristics but not the temporal properties of Ca^{2+} sparks.

IVA regulated RyR2, SERCA2 and NCX1 protein expression in rabbit atriums

The expression of RyR2 and SERCA2 were increased and decreased, respectively, in the hearts treated with IVA (1-10 μM) in a manner of concentration ($n = 4-5$, $p < 0.05$ vs. baseline). NCX1 expression was up-regulated by 10 μM IVA ($n = 4-5$, $p < 0.05$ vs. baseline, Fig 7).

Discussion

The main findings of this study include: (1) Reduction by IVA of intrinsic atrial rate could be attenuated in hearts with increased either vagal activity or late I_{Na} ; (2) IVA prolonged MAPD_{90} , ERP and PRR in atria and decreased the APA and V_{max} in myocytes at relatively low therapeutic concentrations ([?] 0.1 μM) and lengthened QRS and QT intervals at high concentration range (> 3 μM) in isolated hearts; (3) Modulation of IVA on atrial MAPD_{90} and APD were condition dependent, it prolonged $\text{MAPD}_{90}/\text{APD}$ in ACh-treated but shortened $\text{MAPD}_{90}/\text{APD}$ in ATX-II treated hearts or cells, respectively; (4) IVA (0.03-10 μM) induced greater incidence of atrial arrhythmias either at slow heart rate or in the presence of ATX-II or ACh, and DADs in atrial myocytes; (5) IVA increased the frequency, amplitude, FWHM of calcium spark, up-regulated RyR2 and NCX1 protein expression, and down-regulated SERCA2 protein expression, leading to intracellular Ca^{2+} overload.

In denervated rabbit isolated hearts, the intrinsic sinus heart rate was reduced by IVA at therapeutic concentration range, i.e., approximately 0.02-0.05 μM^{14} . The results in this study conform to the findings of previous basic and clinical investigations that IVA inhibits I_{f} in the sinus node to slow sinus rate¹⁵. Meanwhile, IVA also lengthened the PR interval due to the prolongation of the conduction time in the AV node at relative high concentrations, i.e., [?] 1 μM , presumably due to a prolongation of the ERP in the AV node following a prolongation of the APD in the heart (see below) and the increase in the atrial rate due to atrial arrhythmias. Interestingly, in isolated hearts treated with low concentration of ATX-II or ACh to increase atrial late I_{Na} ¹⁶ or vagal activity, the amplitude of HR reduction by IVA would be reduced, which may be result from the slower basal HR by drugs or under pathological conditions of the heart. Further investigation will be needed to clarify the conditions at which the efficacy of IVA on HR would be attenuated.

The MAPD₉₀, ERP and PRR were prolonged by IVA at concentrations higher than the therapeutic range (i.e., 0.02-0.05 μM)¹⁴, consistent with other research in rabbit hearts¹⁷. Previous studies have shown that IVA, at concentrations higher than the therapeutic concentration, blocks I_{Kr} (IC₅₀=2.8 μM)¹⁸, which was attributed to the prolongation of APD in this study. The overt prolongation in the APD by drugs that inhibit I_{Kr} (class III antiarrhythmic drugs, macrolide and quinolone antibiotics) is undesirable, because it is associated with torsade de pointes ventricular tachycardia in the heart¹⁹.

These results support the hypothesis that atrial proarrhythmic risk of IVA was increased in hearts with slow rate, enhanced late I_{Na} and vagal activation. IVA induced much greater incidence of atrial arrhythmias in hearts paced at CL of 570ms than at CL of 350 ms (76.9% vs. 26.1%). In hearts with increased late I_{Na} by ATX-II or ACh to simulate vagal excitation, IVA modulated the MAPD₉₀, lengthened the ERP and PRR, and induced atrial arrhythmias in 44.4% and 61.9% of hearts paced at a fixed CL of 350 ms, suggesting that risk of proarrhythmia by IVA was increased under pathological conditions in the atria. This result is consistent with the findings from clinical studies that the risk of AF is increased by 24% in patients treated with IVA⁹ and that sodium channelopathies are associated with an increased risk of atrial arrhythmias, including AFs²⁰. Wu et al. reported that an increase in late I_{Na} by ATX-II potentiated the proarrhythmic activity of low-risk QT-prolonging drugs²¹. The prolongation of the MAPD caused by drugs that purely inhibit I_{Kr} is synergistically increased in hearts treated with late I_{Na} enhancers²¹. However, drugs that potentially inhibit late I_{Na} cause an increase (i.e., pentobarbital) or sometimes a shortening (such as ranolazine) of the MAPD¹⁶.

I_f is a kind of Na⁺/K⁺ mixed current (a net inward current) and is mainly involved in the automatic depolarization of sinoatrial node cells in phase 4²². IVA decreased the amplitude and V_{max} of an AP without affecting AP duration at relatively low concentration which might be attributed to the inhibitory effect on the I_{Na} of the atrial myocytes. IVA mainly affected the AP duration and triggering activity, i.e., DAD, of atrial cells pretreated with either ACh or ATX-II. When IVA was applied to ATX-II-/ACh-treated cells, APD₃₀, APD₅₀ and APD₉₀ were either shortened or prolonged, indicating that IVA could also affect I_{K1} and I_{KACH} under certain conditions without affecting RMP, APA and V_{max} at low therapeutic concentration range²³. Finally, IVA increased DADs but not EADs in both in the absence and presence of either ACh or ATX-II in atrial myocytes. DAD is related to intracellular calcium overload and abnormal Ca²⁺ handling associated with the increase of Na⁺/Ca²⁺ exchange^{24, 25}.

IVA mainly enhanced the frequency, amplitude and FWHM (spatial characteristics) with little effects on the FDHM (temporal properties) of Ca²⁺ sparks. Ca²⁺ sparks are local Ca²⁺ release events from the sarcoplasmic reticulum (SR), with one spark representing the flux of Ca²⁺ through a single SR release channel or RyR²⁶. Spontaneous Ca²⁺ sparks are thought to play a major role in SR Ca²⁺ leakage, and the frequency, amplitude and FWHM of these sparks are highly dependent on the Ca²⁺ concentration in the SR ([Ca²⁺]_{SR})²⁷. In rabbit ventricular cells, a higher [Ca²⁺]_{SR} (>600 μM) led to increased calcium spark amplitude and width, Ca²⁺ sparks became a significant pathway of SR Ca²⁺ leakage, and Ca²⁺ sparks disappeared at \sim 300 μM [Ca²⁺]_{SR}, the Ca²⁺ spark termination threshold²⁸.

Increased Ca²⁺ signaling instability occurs in AF^{29, 30} and contributes to atrial arrhythmia and the maintenance of AF²⁴, especially in patients with cardiovascular diseases, including heart failure and ischemic heart disease, etc. These mechanisms may be attributed to the change in the Ca²⁺ release flux as the Ca²⁺ gradient across the SR membrane or to luminal Ca²⁺-dependent RyR regulation³¹. Diastolic Ca²⁺ sparks are spontaneous bouts of localized inter-RyR Ca²⁺-induced Ca²⁺ release (CICR) that are likely triggered by a rare stochastic opening of a single RyR channel. A spark occurs if the RyR Ca²⁺ flux amplitude mediated by that rare channel opening is sufficient to drive inter-RyR CICR. The results in this study indicated that IVA increased the Ca²⁺ release and Ca²⁺-based arrhythmogenic substrate may contribute to the initiation of AF caused by IVA.

Drug-induced AF of IVA application may be atrial DADs-related and activation of Ca²⁺ sparks, which contribute to the AF trigger. The differences in calcium instability between cells from atria and pulmonary sleeve need to be determined because intracellular Ca²⁺ was reported to be reduced in pulmonary veins.

Predominant resource of increased intracellular calcium is yet to be fully determined in this study and is worth of further investigation.

When $[Ca^{2+}]_i$ increases due to spontaneous Ca^{2+} release events, a Ca^{2+} -based membrane current is activated during diastole. This arrhythmogenic transient inward current (I_{ti}), which is carried by the sarcolemmal NCX, is responsible for DAD generation. Enhancement of late I_{Na} is one of the causes to increase $[Ca^{2+}]_i$ because it increase $[Na^+]_i$ and then $[Ca^{2+}]_i$ through NCX to facilitate DAD formation and therefore was used in this project to augment the proarrhythmic risk of IVA. When DADs are sufficiently large, they can trigger extrasystole. Additionally, Ca^{2+} -activated I_{ti} can occur during repolarization and then contribute to triggered activities, which trigger extrasystoles and atrial tachyarrhythmias.

Phosphorylation-mediated RyR2 sensitization is implicated in unstable Ca^{2+} signaling, i.e., increased Ca^{2+} spark frequency and diastolic Ca^{2+} leak in the genesis of AF. Ca^{2+} -based arrhythmic events caused by unstable $[Ca^{2+}]_i$ signaling are mediated by intracellular Ca^{2+} waves and Ca^{2+} -activated inward currents. Ca^{2+} overload (i.e., increased $[Ca^{2+}]_{SR}$) increases the sensitivity of the RyR2s to activation by cytosolic $[Ca^{2+}]_i$ ³². This higher $[Ca^{2+}]_i$ sensitivity leads to an increased probability of spontaneous Ca^{2+} sparks and Ca^{2+} waves.

Drug induced AF, including both cardiovascular and non-cardiovascular agents, may have diverse mechanisms³³. Adequate understanding of these mechanisms underlying the increased risk of drug induced AF is critical for the prevention and management of this kind of AF. The results in this study indicated that intracellular Ca^{2+} overload associated triggered activities and the reduction of HR by IVA may have synergistic effects to increase the risk of IVA induced AF in the heart. Further study will be needed to determine how does the IVA to increase the calcium release from the sarcoplasm reticulum and the characteristics of IVA induced AF under different pathophysiological conditions.

Conclusions

IVA reduces sinus rate, evokes Ca^{2+} sparks and causes DAD-driven trigger activities to induce or increase the risk of AF in condition-dependent manners. A slow heart rate, enhancement of vagal activity and late I_{Na} facilitate the proarrhythmic effects of IVA in the heart.

Declaration of Conflicting Interests

The authors declare that there is no conflict of interest.

Acknowledgments

This study was funded by Chinese National Natural Science Foundation (Grant NOs. 81270253, 81670304, 81770325 and 81930105).

References:

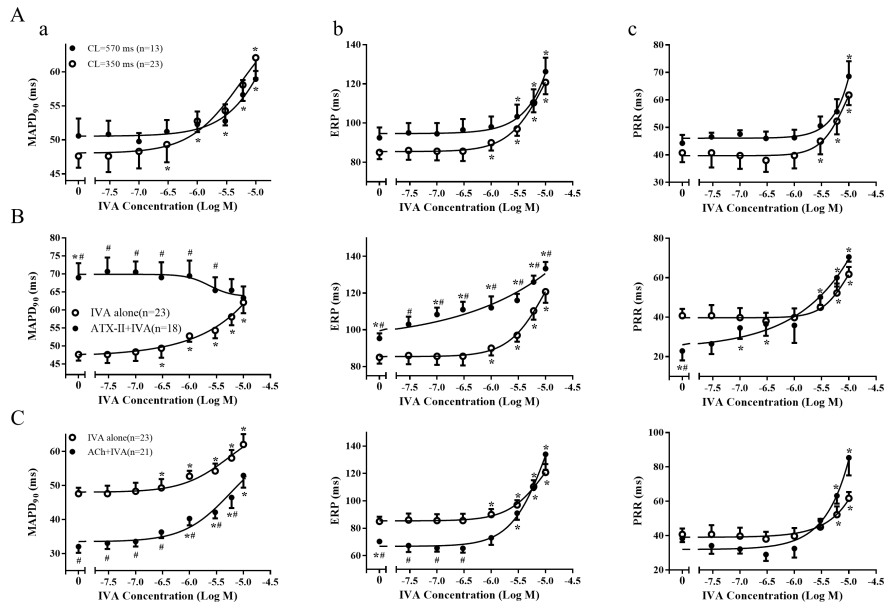
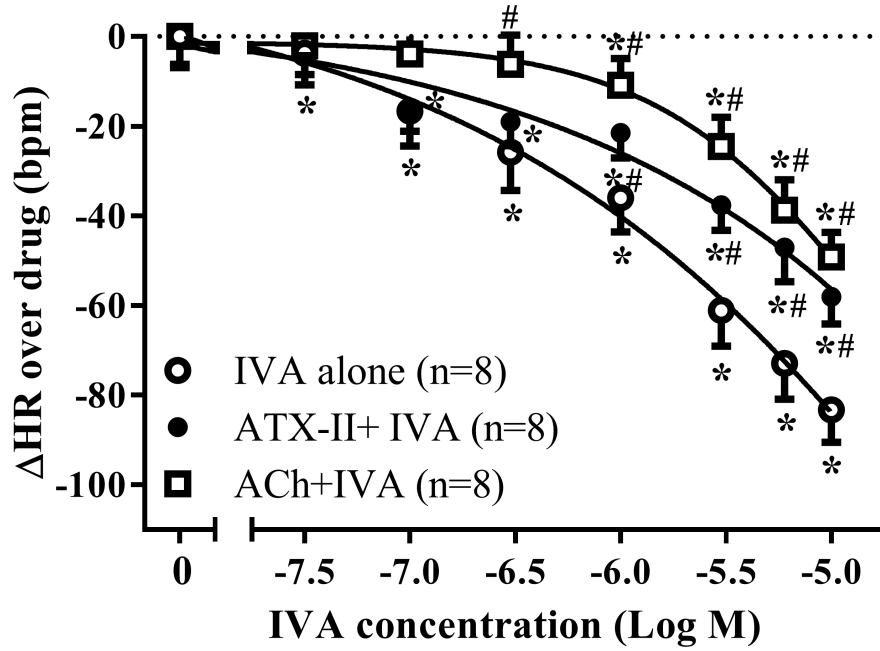
- 1 van der Hooft CS, Heeringa J, van Herpen G, Kors JA, Kingma JH, Stricker BH: Drug-induced atrial fibrillation. *J AM COLL CARDIOL* 2004; 44:2117-2124.
- 2 Kaakeh Y, Overholser BR, Lopshire JC, Tisdale JE: Drug-Induced Atrial Fibrillation. *DRUGS* 2012; 72:1617-1630.
- 3 Lei M, Wu L, Terrar DA, Huang CLH: Modernized Classification of Cardiac Antiarrhythmic Drugs. *CIRCULATION* 2018; 138:1879-1896.
- 4 Cappato R, Castelvécchio S, Ricci C, Bianco E, Vitali-Serdoz L, Gneccchi-Rusccone T, Pittalis M, De Ambroggi L, Baruscotti M, Gaeta M, Furlanello F, Di Francesco D, Lupo PP: Clinical efficacy of ivabradine in patients with inappropriate sinus tachycardia: a prospective, randomized, placebo-controlled, double-blind, crossover evaluation. *J AM COLL CARDIOL* 2012; 60:1323-1329.
- 5 Chow SL, Page RN, Depre C: Role of ivabradine and heart rate lowering in chronic heart failure: guideline update. *Expert Rev Cardiovasc Ther* 2018; 16:515-526.

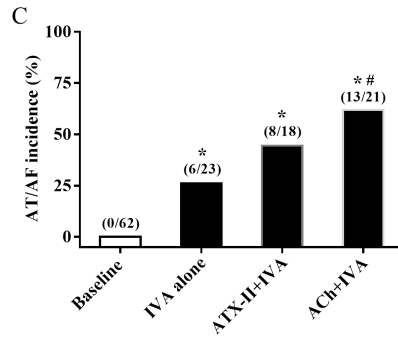
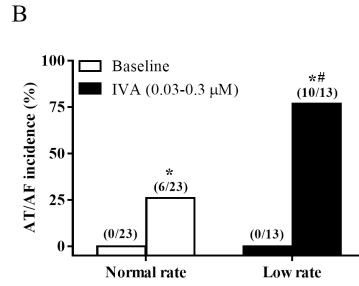
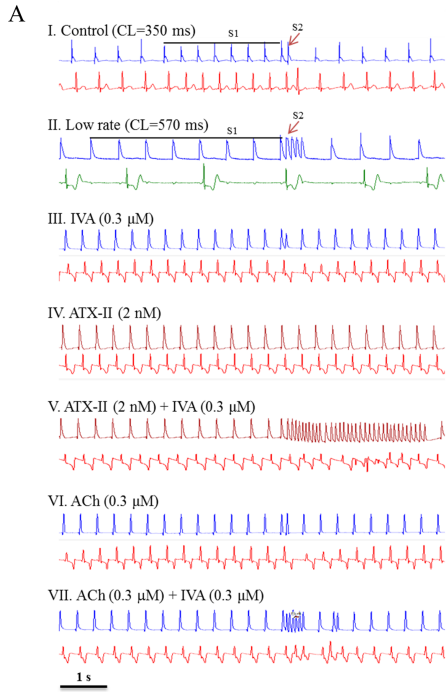
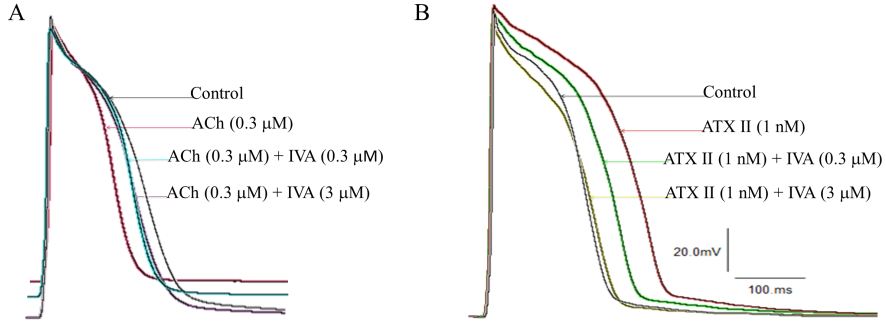
- 6 Dvir D, Battler A: Conventional and novel drug therapeutics to relief myocardial ischemia. *Cardiovasc Drugs Ther* 2010; 24:319-323.
- 7 Wang J, Yang YM, Li Y, Zhu J, Lian H, Shao XH, Zhang H, Fu YC, Zhang LF: Long-term treatment with ivabradine in transgenic atrial fibrillation mice counteracts hyperpolarization-activated cyclic nucleotide gated channel overexpression. *J Cardiovasc Electrophysiol* 2019; 30:242-252.
- 8 Burashnikov A, Antzelevitch C: Reinduction of atrial fibrillation immediately after termination of the arrhythmia is mediated by late phase 3 early afterdepolarization-induced triggered activity. *CIRCULATION* 2003; 107:2355-2360.
- 9 Tanboga IH, Topcu S, Aksakal E, Gulcu O, Aksakal E, Aksu U, Oduncu V, Ulusoy FR, Sevimli S, Kaymaz C: The Risk of Atrial Fibrillation With Ivabradine Treatment: A Meta-analysis With Trial Sequential Analysis of More Than 40000 Patients. *CLIN CARDIOL* 2016; 39:615-620.
- 10 Wu L, Rajamani S, Shryock JC, Li H, Ruskin J, Antzelevitch C, Belardinelli L: Augmentation of late sodium current unmasks the proarrhythmic effects of amiodarone. *CARDIOVASC RES* 2008; 77:481-488.
- 11 Zhang Q, Ma JH, Li H, Wei XH, Zheng J, Li G, Wang CY, Wu Y, He QH, Wu L: Increase in CO₂ levels by upregulating late sodium current is proarrhythmic in the heart. *HEART RHYTHM* 2019; 16:1098-1106.
- 12 Picht E, Zima AV, Blatter LA, Bers DM: SparkMaster: automated calcium spark analysis with ImageJ. *Am J Physiol Cell Physiol* 2007; 293:C1073-C1081.
- 13 Zhang Q, Ma J, Li H, Wei X, Zheng J, Li G, Wang C, Wu Y, He Q, Wu L: Increase in CO₂ levels by upregulating late sodium current is proarrhythmic in the heart. *HEART RHYTHM* 2019; 16:1098-1106.
- 14 Sheldon RS, Grubb BP, Olshansky B, Shen W, Calkins H, Brignole M, Raj SR, Krahn AD, Morillo CA, Stewart JM, Sutton R, Sandroni P, Friday KJ, Hachul DT, Cohen MI, Lau DH, Mayuga KA, Moak JP, Sandhu RK, Kanjwal K: 2015 Heart Rhythm Society Expert Consensus Statement on the Diagnosis and Treatment of Postural Tachycardia Syndrome, Inappropriate Sinus Tachycardia, and Vasovagal Syncope. *HEART RHYTHM* 2015; 12:e41-e63.
- 15 Ceconi C, Cargnoni A, Francolini G, Parinello G, Ferrari R: Heart rate reduction with ivabradine improves energy metabolism and mechanical function of isolated ischaemic rabbit heart. *CARDIOVASC RES* 2009; 84:72-82.
- 16 Chu Y, Yang Q, Ren L, Yu S, Liu Z, Chen Y, Wei X, Huang S, Song L, Zhang P, Ma J, Wu L: Late Sodium Current in Atrial Cardiomyocytes Contributes to the Induced and Spontaneous Atrial Fibrillation in Rabbit Hearts. *J Cardiovasc Pharmacol* 2020; 76:437-444.
- 17 Suenari K, Cheng CC, Chen YC, Lin YK, Nakano Y, Kihara Y, Chen SA, Chen YJ: Effects of ivabradine on the pulmonary vein electrical activity and modulation of pacemaker currents and calcium homeostasis. *J Cardiovasc Electrophysiol* 2012; 23:200-206.
- 18 DiFrancesco D, Camm JA: Heart rate lowering by specific and selective I(f) current inhibition with ivabradine: a new therapeutic perspective in cardiovascular disease. *DRUGS* 2004; 64:1757-1765.
- 19 Wu L, Ma J, Li H, Wang C, Grandi E, Zhang P, Luo A, Bers DM, Shryock JC, Belardinelli L: Late sodium current contributes to the reverse rate-dependent effect of IKr inhibition on ventricular repolarization. *CIRCULATION* 2011; 123:1713-1720.
- 20 Martin RI, Pogoryelova O, Koref MS, Bourke JP, Teare MD, Keavney BD: Atrial fibrillation associated with ivabradine treatment: meta-analysis of randomised controlled trials. *HEART* 2014; 100:1506-1510.
- 21 Wu L, Rajamani S, Li H, January CT, Shryock JC, Belardinelli L: Reduction of repolarization reserve unmasks the proarrhythmic role of endogenous late Na(+) current in the heart. *Am J Physiol Heart Circ Physiol* 2009; 297:H1048-H1057.

- 22 Kleinbongard P, Gedik N, Witting P, Freedman B, Klocker N, Heusch G: Pleiotropic, heart rate-independent cardioprotection by ivabradine. *Br J Pharmacol* 2015; 172:4380-4390.
- 23 van der Heyden MA, Jespersen T: Pharmacological exploration of the resting membrane potential reserve: Impact on atrial fibrillation. *EUR J PHARMACOL* 2016; 771:56-64.
- 24 Voigt N, Li N, Wang Q, Wang W, Trafford AW, Abu-Taha I, Sun Q, Wieland T, Ravens U, Nattel S, Wehrens XH, Dobrev D: Enhanced sarcoplasmic reticulum Ca²⁺ leak and increased Na⁺-Ca²⁺ exchanger function underlie delayed afterdepolarizations in patients with chronic atrial fibrillation. *CIRCULATION* 2012; 125:2059-2070.
- 25 Voigt N, Heijman J, Wang Q, Chiang DY, Li N, Karck M, Wehrens X, Nattel S, Dobrev D: Cellular and molecular mechanisms of atrial arrhythmogenesis in patients with paroxysmal atrial fibrillation. *CIRCULATION* 2014; 129:145-156.
- 26 Cheng H, Lederer WJ, Cannell MB: Calcium sparks: elementary events underlying excitation-contraction coupling in heart muscle. *SCIENCE* 1993; 262:740-744.
- 27 Zima AV, Bovo E, Bers DM, Blatter LA: Ca²⁺ spark-dependent and -independent sarcoplasmic reticulum Ca²⁺ leak in normal and failing rabbit ventricular myocytes. *J Physiol* 2010; 588:4743-4757.
- 28 Satoh H, Blatter LA, Bers DM: Effects of [Ca²⁺]_i, SR Ca²⁺ load, and rest on Ca²⁺ spark frequency in ventricular myocytes. *Am J Physiol* 1997; 272:H657-H668.
- 29 Hove-Madsen L, Llach A, Bayes-Genis A, Roura S, Rodriguez FE, Aris A, Cinca J: Atrial fibrillation is associated with increased spontaneous calcium release from the sarcoplasmic reticulum in human atrial myocytes. *CIRCULATION* 2004; 110:1358-1363.
- 30 Neef S, Dybkova N, Sossalla S, Ort KR, Fluschnik N, Neumann K, Seipelt R, Schondube FA, Hasenfuss G, Maier LS: CaMKII-dependent diastolic SR Ca²⁺ leak and elevated diastolic Ca²⁺ levels in right atrial myocardium of patients with atrial fibrillation. *CIRC RES* 2010; 106:1134-1144.
- 31 Gyorke I, Gyorke S: Regulation of the cardiac ryanodine receptor channel by luminal Ca²⁺ involves luminal Ca²⁺ sensing sites. *BIOPHYS J* 1998; 75:2801-2810.
- 32 Wier WG, Cannell MB, Berlin JR, Marban E, Lederer WJ: Cellular and subcellular heterogeneity of [Ca²⁺]_i in single heart cells revealed by fura-2. *SCIENCE* 1987; 235:325-328.
- 33 Tamargo J, Caballero R, Delpon E: Drug-induced atrial fibrillation. *EXPERT OPIN DRUG SAF* 2012; 11:615-634.

Hosted file

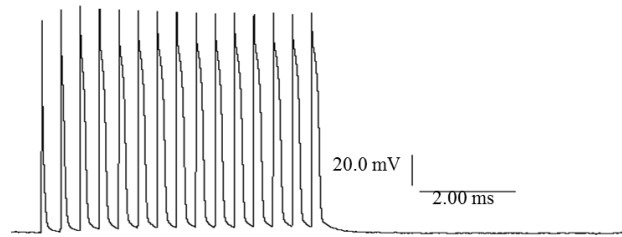
Table.docx available at <https://authorea.com/users/611037/articles/710544-atrial-proarrhythmias-of-ivabradine-by-inducing-intracellular-calcium-overload-and-delayed-afterdepolarizations-in-rabbit-heart>



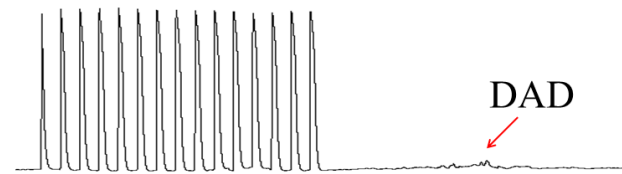


A

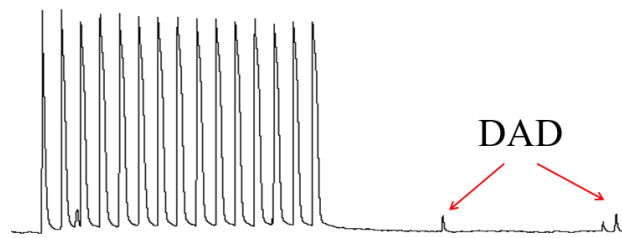
I. Baseline



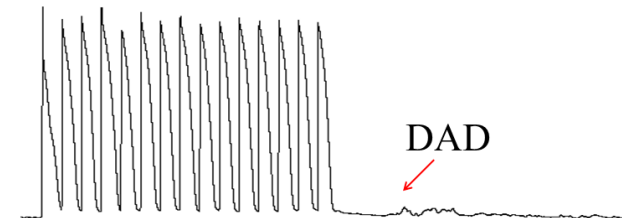
II. IVA alone (0.3-3 μ M)



III. ACh (0.3 μ M) + IVA (0.3-3 μ M)



IV. ATX II (1 nM) + IVA (0.3-3 μ M)



B

